Applied Catalysis A: General 485 (2014) 207–213

Contents lists available at ScienceDirect

Applied Catalysis A: General

journal homepage: www.elsevier.com/locate/apcata

Titania-based photocatalytic degradation of two nucleotide bases, cytosine and uracil

L. Elsellami[a,b], K. Sahel[a,c], F. Dappozze[a], S. Horikoshi[d], A. Houas[b], C. Guillard[a,*]

[a] IRCELYON, CNRS UMR 5256/Université Lyon1, 2 av. Albert Einstein, Villeurbanne Cedex, 69626, France
[b] Unité de recherché Catalyse et Matériaux pour l'Environnement et les Procédés URCMEP (UR11ES85) Campus Universitaire Hatem BETTAHAR-Cité Erriadh, 6072 Gabes, Tunisia
[c] Laboratoire Physico-chimie des Matériaux, Catalyse et Environnement, Département de Chimie, Faculté des Sciences, Université des Sciences et de la Technologie d'Oran (USTO) , Oran, Algeria
[d] Sophia University, Faculty of Science and Technology, Department of Materials and Life Sciences, 7-1 Kioicho, Chiyodaku, Tokyo, Japan

ARTICLE INFO

Article history:
Received 23 March 2014
Received in revised form 22 July 2014
Accepted 30 July 2014
Available online 7 August 2014

Keywords:
Cytosine
Uracil
TiO_2
Photocatalysis
Reaction mechanism

ABSTRACT

The photocatalytic degradation of two components of DNA and RNA, cytosine ($C_4H_5N_3O$) and uracil ($C_4H_4N_2O_2$) differing only by the presence of an amine or a carbonyl group was investigated in the presence of UV-irradiated TiO_2 aqueous suspensions. The adsorption in the dark and under UV-A conditions, the photolysis, the kinetics of degradation, the fate of nitrogen and the identification of some intermediate products were investigated. The impact of pyrimidine cycles on the coverage of TiO_2 under UV-A, the effect of NH_2 substituent on the oxidation products and mineralization and the importance of carbonyl and amine groups on the fate of nitrogen atoms were evaluated. Electronic density was used to propose a possible chemical pathway. The comparison of the disappearance and mineralization rates in the photocatalytic process was discussed.

1. Introduction

Heterogeneous photocatalysis is an advanced oxidation process (AOT) allowing efficient production of hydroxyl radicals under appropriate conditions depending of the photocatalyst used. These radicals have an oxidizing power much greater than traditional oxidants. They are capable of partially or completely mineralizing most of organic compounds [1–4]. The most widely used catalyst is TiO_2 because of its relative high photocatalytic activity, its stability, its availability and its relative low cost [5–7]. Under UV-light, titanium dioxide is an extremely powerful oxidant able to break the carbon chains. The pollutants are mineralized into water and carbon dioxide.

Pyrimidine compounds are largely found in biomolecules and agrochemicals [8]. Several studies deal with the photocatalytic degradation of pyrimidine compounds [9–16]. They mainly focused on the degradation mechanism of DNA bases (uracil, thymine, and cytosine) and on ionic effects. Such studies are highly relevant to water and cancer treatments.

The pyrimidine bases, issued from the decomposition of nucleic acids, are present in natural waters and sediments [17]. All these compounds may be considered as water pollutants which can be eliminated by photocatalysis [12,14,16].

Jaussaud et al. [18] and Dhananjeyan et al. [11] have studied the influence of different parameters such as concentration of pollutant, concentration of catalyst, pH, $CdCl_2$, oxygen concentration, influence of metallic ions on the photodegradation of pyrimidine bases in the presence of titanium dioxide. Horikoshi et al. [16] have studied the photomineralization pathways of pyrimidine and purine bases by UVA/UVB illuminated TiO_2 and the respective rates of formation of NH_4^+ and NO_3^- ions. Recently, Li at al [15] have compared the photocatalytical and photo-electrochemical degradation mechanism of these nucleotide bases. Singh et al. [19] gave a detailed kinetic study of uracil and 5-bromouracil. They deduced that TiO_2 can efficiently catalyze the photomineralization of uracil and 5-bromouracil. They also found that photocatalyst Degussa P25 showed the highest photocatalytic activity and they suggested that the addition of electron acceptors such as hydrogen peroxide and potassium bromate can enhance the decomposition.

Our objective is a better understanding of the photocatalytic mechanism of the elimination of uracil and cytosine, which are the simplest molecules constituting the microorganisms (DNA, RNA, proteins, etc.).

* Corresponding author at: 2 avenue Albert Einstein, F-69626 Villeurbanne, France. Tel.: +33 472445316; fax: +33 472445399.
E-mail address: chantal.guillard@ircelyon.univ-lyon1.fr (C. Guillard).

http://dx.doi.org/10.1016/j.apcata.2014.07.043
0926-860X/

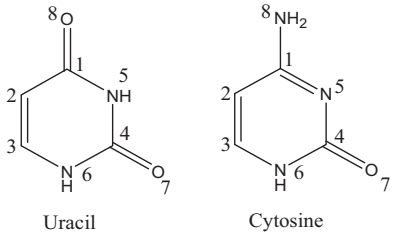

Fig. 1. Structural formulas of uracil and cytosine.

2. Experimental

2.1. Reagents and chemicals

Pyrimidine bases uracil (Ura: $C_4H_4N_2O_2$) and cytosine (Cyt: $C_4H_5N_3O$) (99% purity) were purchased from SIGMA-Aldrich and used as received. Their formulae are given in Fig. 1. Water used for preparation of samples was ultra-pure water, filtered through a milli-Q PLUS 185 water system. The photocatalyst was titanium dioxide Degussa P-25 (particle size, 20–30 nm; crystal structure, 80% anatase and 20% rutile; surface area, 50 $m^2\,g^{-1}$).

2.2. Reactor and light source

The aqueous suspensions were irradiated in a 100 mL open cylindrical reactor whose base contained an optical window with a surface area of about 12.6 cm^2. The output of a Philips HPK 125 W high mercury lamp was filtered through a circulating water cell (thickness = 2.2 cm), avoiding the solution warming by IR, and a Corning 0.52 mW/cm^2 filter to remove radiation with wavelength below 340 nm. The radiant flux was measured using a VLX-3 W radiometer with a detector CX-365 (355–375 nm).

2.3. Photocatalytic experiments

A volume of 20 mL of uracil and cytosine solution with different concentrations containing a concentration of 1.25 $g\,L^{-1}$ of TiO_2, sufficient to absorb all photons entering the photoreactor was used [20]. The degradation was carried out at room temperature (T = 25 °C) and at natural pH (pH 5). The suspension was first stirred in the dark until equilibrium adsorption was achieved. Then, the solution was irradiated at $\lambda > 340$ nm and a radiant flux equal to 3.5 mW/cm^2. Samples taken at different times of irradiation were filtered through 0.45 μm Waters filters to remove TiO_2 particles before analyses.

2.4. Methods of analysis

The degradation of uracil and cytosine were followed by HPLC with a Varian System equipped with a Varian Prostar 230 isocratic pump and a Varian Prostar 330 Diode Area Detector adjusted at 254 nm. A Hypersil BDS C18 reverse phase column (125 mm long, 4 mm diameter) was used. The mobile phase was constituted by 90% of ultra-pure water containing 62 μL H_3PO_4 at pH 3 and 10% of methanol. The flow rate was 0.8 mL min^{-1}.

Mineralization of pyrimidine bases was monitored by determination of Total Organic Carbon (TOC) concentrations by direct injection of the filtered samples using TOC-VCSH Shimadzu and ASI-V Shimadzu sampler.

The carboxylic acids formed were analyzed by LC using a Varian Prostar 230 pump, a Varian Prostar 325 UV detector (detection at 210 nm), and a Transgenomic Icsep Coregel 87H (300 mm × 4.6 mm) column. The flow rate was 0.7 mL min^{-1}. The injection volume was 100 μL and the mobile phase was H_2SO_4 (5×10^{-3} mol L^{-1}).

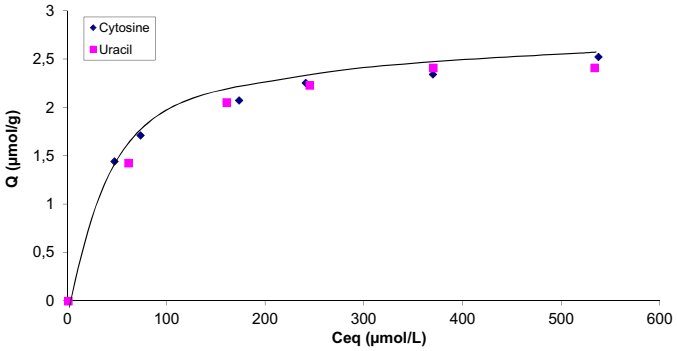

Fig. 2. Amounts of cytosine and of uracil adsorbed per gram of TiO_2 as a function of the equilibrium concentration C_{eq} on TiO_2 Degussa P25 (1.25 $g\,L^{-1}$).

The formation of nitrate ions was monitored using ionic chromatography with a Dionex DX-120 pump and conductivity detector, and an IonPac AS14A (250mm × 4 mm) column. The flow rate was 1 mL min^{-1} and the mobile phase was an alkaline buffer ($NaHCO_3$ (1.0 mmol L^{-1}) + Na_2CO_3 (8.0 mmol L^{-1})).

The formation of ammonium ions was also followed using ionic chromatography with a Dionex DX-120 pump and conductivity detector. The column was a CS 12A (250 mm × 4 mm). The flow rate was 1 mL min^{-1} and the mobile phase was H_2SO_4 solutions containing 610 μL L^{-1} of pure sulfuric acid.

For all analyses the error bars are about 5%.

Computer simulations with MOPAC allowed to calculate the frontier electron density used to determine the positions of •OH radical attack in uracil and cytosine.

3. Results and discussion

3.1. Adsorption

In order to ensure that the adsorption process reached equilibrium, different concentrations of uracil and cytosine were stirred in the dark in the presence of TiO_2 and analysed as a function of time. In both cases, the uracil and cytosine adsorptions reached equilibrium after about 60 min.

Fig. 2(a) represents the amounts (μmol g^{-1}) of cytosine and uracil adsorbed per gram of TiO_2 as a function of the cytosine and uracil equilibrium concentration (C_{eq}). In dark conditions, the amounts of cytosine and uracil adsorbed on the TiO_2 surface (Q_{eq}) increase with the equilibrium concentration until reaching a plateau. The amounts of cytosine and of uracil adsorbed are identical, probably because of their similar formulae. The maximum coverage of cytosine and uracil is about 0.03 molecule nm^{-2}. This represents about 0.6% of the maximum coverage in OH surface groups equal to 5 OH/nm^2 [21]. This value is similar to values found for molecules containing aromatic cycles such as tryptophan, phenylalanine [22,23].

As for the majority of organic compounds [22–27], the adsorption isotherms of cytosine and uracil can be modelled using the Langmuir approach:

$$Q_{eq} = K_{ads} Q_{max} C_{eq} (1 + K_{ads} C_{eq})$$

Q_{eq} is the adsorbed quantity of pollutant on the photocatalyst at the equilibrium (μmol g^{-1}), K_{ads} is the adsorption constant (L μmol^{-1}), Q_{max} is the maximum amount to be adsorbed (μmol g^{-1}), and C_{eq} is the concentration of the compound at the adsorption equilibrium (μmol L^{-1}). The values of the Langmuir parameters for cytosine and uracil are presented in Table 1.

Table 1
Langmuir parameters for cytosine and uracil adsorption.

Compounds	K_{ads} (L μmol^{-1})	Q_{max} (μmol g^{-1})	Q_{max} (molecule nm^{-2})
Cytosine	0.024	2.5	0.03
Uracil	0.018	2.5	0.03

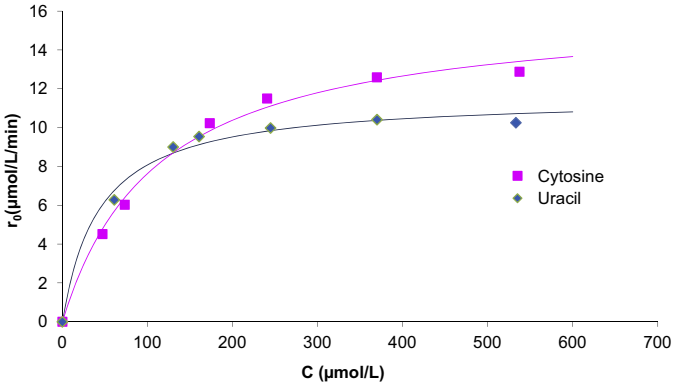

Fig. 3. Variations of the initial rates of disappearance of uracil and of cytosine as a function of the concentration in solution (C). The lines are fits to the Langmuir–Hinshelwood model.

Table 2
Langmuir–Hinshelwood constants obtained under UV conditions.

	k (μmol L^{-1} min^{-1})	$K_{ads(UV)}$ (L μmol^{-1})
Uracil	11	0.022
Cytosine	16	0.008

3.2. Photodegradation of uracil and cytosine

We first checked that the direct photolysis was negligible.

The initial rates of disappearance of uracil and cytosine are reported as a function of the concentrations of uracil and cytosine in solution (*C*) (Fig. 3). Until a concentration of about 100-120 μmol L^{-1}, the initial rate is proportional to the uracil and cytosine concentration in solution ($r = kK_{ads(UV)}C$) indicating that the degradation of uracil and cytosine follows first-order kinetics at low concentration [28].

Subsequently, the initial rate became independent of uracil and cytosine concentration. This phenomenon is expected from Langmuir–Hinshelwood type kinetics [29,30] where $r = kK_{ads(UV)}C/(1 + K_{ads(UV)}C)$, since the product of the adsorption constant, $K_{ads(UV)}$, by the concentration, cannot be neglected with respect to one in the denominator of *r* at higher concentrations.

$K_{ads(UV)}$ and *k* can be determined by the least squares method where *k* is the rate constant (μmol L^{-1} min^{-1}) and $K_{ads(UV)}$ is the adsorption constant under UV conditions (L μmol^{-1}). The values of $K_{ads(UV)}$ obtained under UV conditions and the values of rate constant *k* are listed in Table 2. From the value of $K_{ads(UV)}$, the coverage ($\theta = K_{ads(UV)}C/(1 + K_{ads(UV)}C)$ under UV was determined.

The coverages of uracil and cytosine in the dark and under UV are given in Fig. 4.

The coverages of uracil under UV and in the dark are similar, whereas in the case of cytosine an important difference was observed. This behaviour can be explained considering the electrical charge of the molecule. Actually, since the p*K* of uracil is 9.3, at natural pH (pH 5), uracil is always neutral, whereas at this pH, cytosine (p*K* 4.2 and 9.3) is positively charged (Fig. 5). It means that under UV, TiO_2 surface is modified and becomes charged, modifying the adsorption of non-neutral molecules. At same coverage, a higher amount of cytosine was found present on TiO_2 surface, leading to a higher disappearance rate.

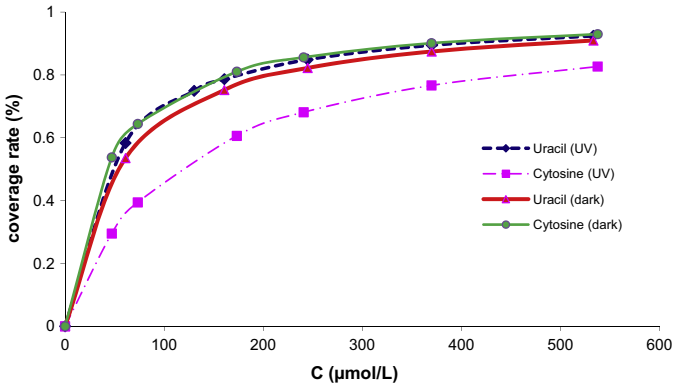

Fig. 4. Reactant coverages in the dark and under UV as a function of uracil and cytosine equilibrium concentrations (*C*).

Table 3
Radical frontier density of cytosine and of uracil.

Atoms	Cytosine radical frontier density	Uracil radical frontier density
C1	0.303	0.211
C2	0.457	0.578
C3	0.380	0.473
C4	0.080	0.104
N5	0.120	0.069
N6	0.301	0.297
O7	0.087	0.096
N8	0.270	/
O8	/	0.165

At similar coverage under UV, cytosine is more quickly degraded than uracil (Fig. 6). This behaviour can be explained considering the presence of donor NH_2 group activating the attack of OH radical.

3.3. Organic carbon mineralization

Mineralization of organic carbon was followed by measuring the TOC evolution during the photocatalytic degradation of uracil and cytosine as shown in Fig. 7. The comparison of mineralization curves shows that at same concentration, uracil is about twice as rapidly mineralized than cytosine. More than 21 h and 41 h were necessary to respectively mineralized more than 99% of organic carbon.

On the basis of the evolution of initial TOC, the presence of the amine group seems to decrease the rate of the decarboxylation and therefore the opening of the cycle. The twice higher decarboxylation rate of uracil could be explained by a more rapid opening of cycle. Actually, considering the radical frontier density (Table 3) before opening the cycle, several hydroxylations of the cycle should be observed, mainly at carbon C2, which has the higher electronic density and also at C3, on nitrogen N6 and finally at C1. In the case of uracil, the hydroxylation on C1 should allow the opening of the cycle whereas in the case of cytosine another step is necessary.

Fig. 8 indicates that after more than 95% of disappearance of cytosine and of uracil, only 15% and 30% of TOC have been mineralized from uracil and cytosine respectively.

The mineralization of uracil is faster compared to that of cytosine whereas the opposite was observed for the initial degradation rates. The initial disappearance rates of parent molecules are not sufficient to determine the efficiency of photocatalytic process. Actually, degradation rates of one parent molecule do not necessarily correlate with total organic carbon removal.

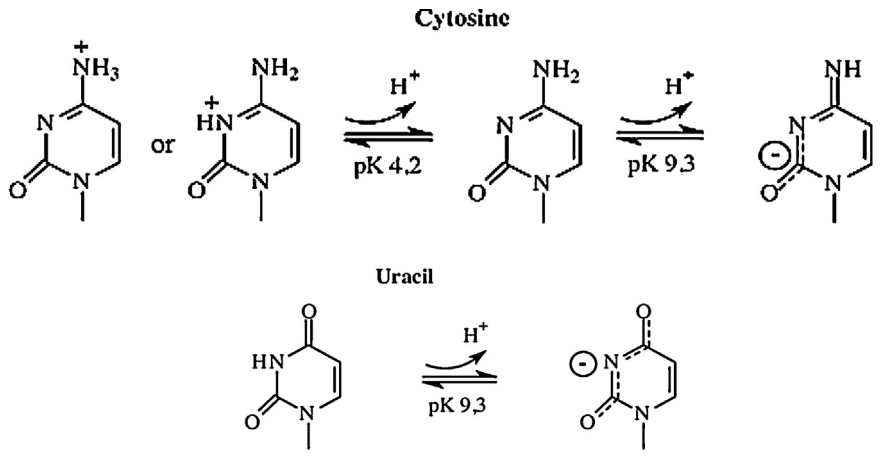

Fig. 5. Ionization states of cytosine and of uracil as a function of pH.

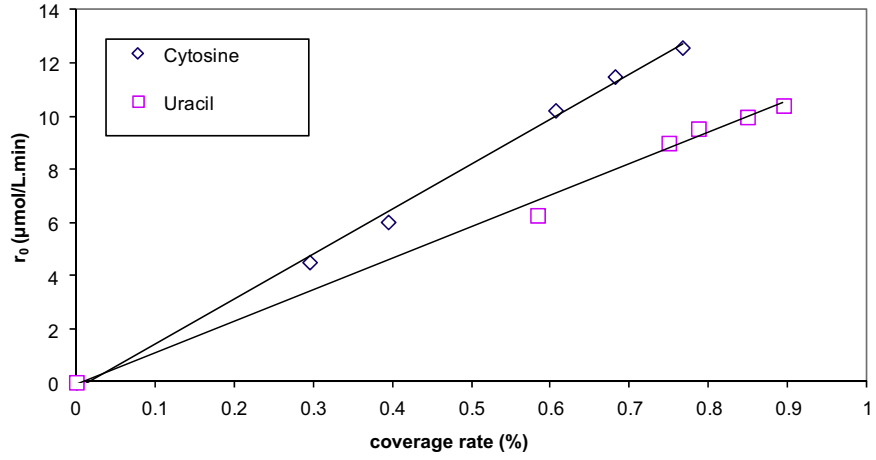

Fig. 6.

3.4. Nitrogen mineralization

The formation of NO_3^- and NH_4^+ from cytosine and uracil show that the presence of primary amine function on the ring completely modifies the proportion of NH_4^+/NO_3^- ions released into the solution (Fig. 9a and b).

In the case of cytosine, NH_4^+ ions are formed initially, whereas the formation of nitrate ions occurs only after the total

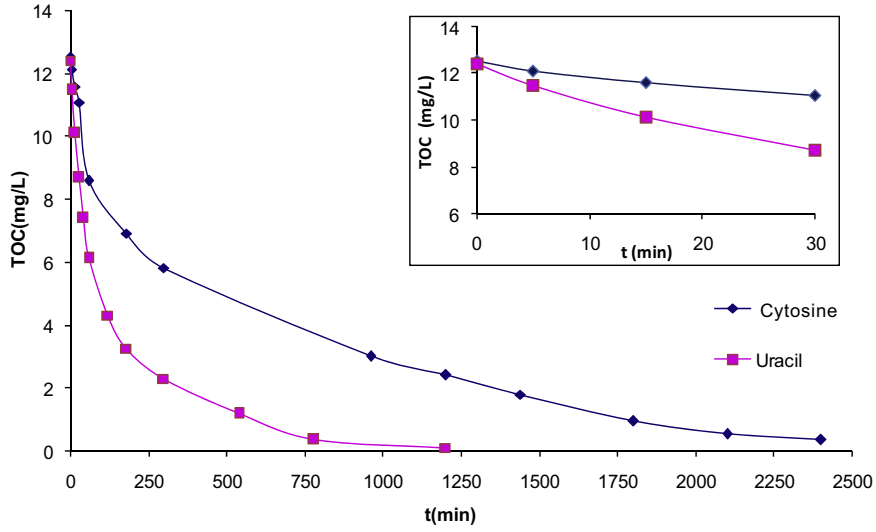

Fig. 7. Kinetics of the total organic carbon (TOC) disappearance during uracil and cytosine degradation with identical initial concentrations ($[uracil]_0 = [cytosine]_0 = 245\ \mu mol\ L^{-1}$).

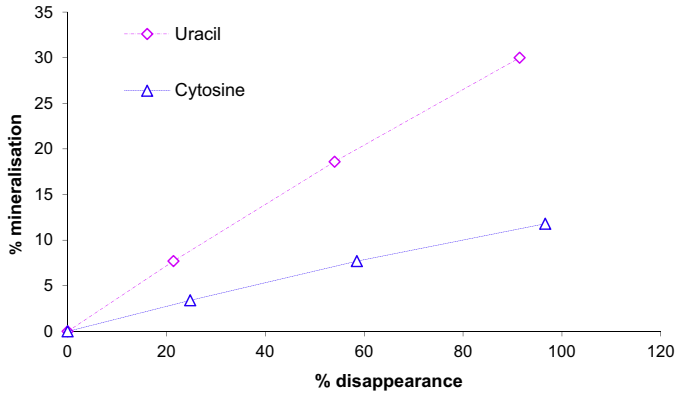

Fig. 8. Percentages of uracil and cytosine mineralization as a function of the percentage of their disappearance.

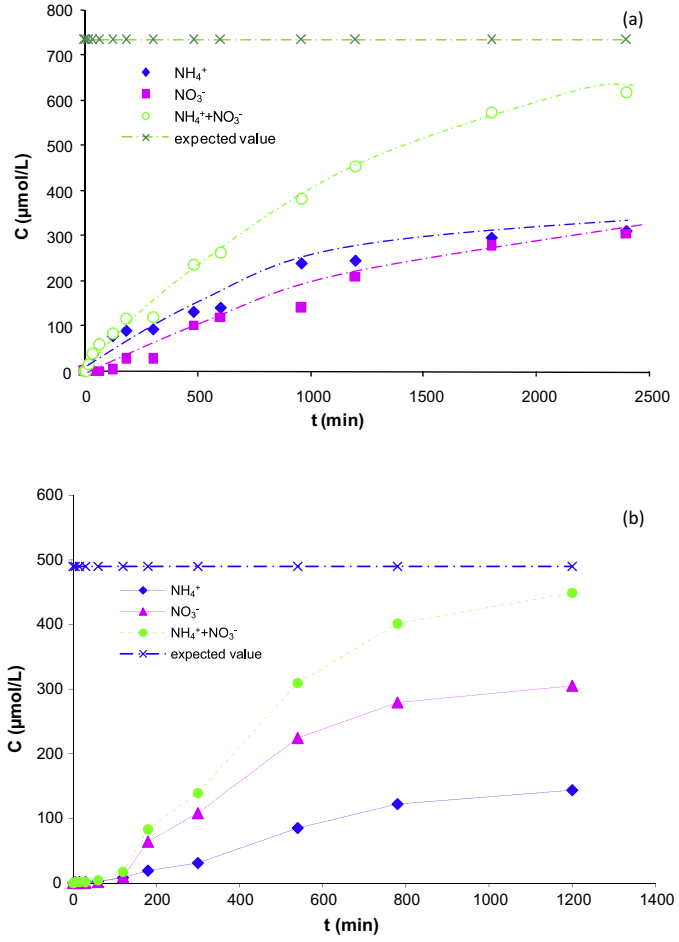

Fig. 9. Formation of ammonium and nitrate ions as a function of irradiation time during the degradation of (a) cytosine and (b) uracil.

disappearance of cytosine (about 2 h) indicating that nitrate ions are not primary oxidation products. After an irradiation time of 40 h, more than 82% of nitrogen initially present in cytosine was converted into ammonium and nitrate ions. The more important formation of NH_4^+ ions is in agreement with the work of Hidaka and co-workers on different amino acids [31,32] and with our previous work showing that the amine group is mainly transformed into ammonium at the start of reaction [24,33]. Actually, the oxidation degree of nitrogen in amine groups and in ammonium is equal to −3. Fig. 10 represents the formation of NH_4^+ ions as a function

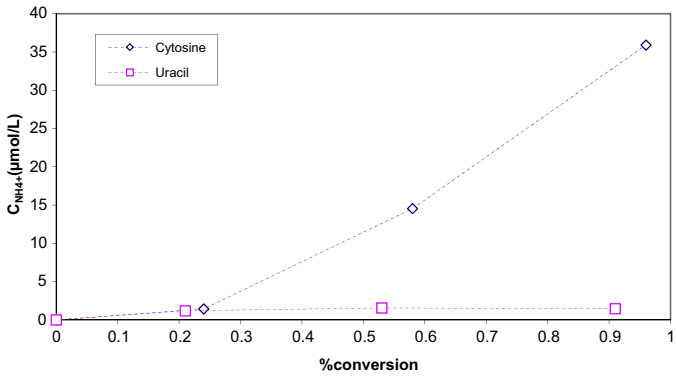

Fig. 10. Formation of ammonium as a function of cytosine and of uracil conversions (in %).

of the % of cytosine disappearance indicates that NH_4^+ ions are not formed from the beginning of degradation and that the hydroxylation of C1 in cytosine, contributing to the breaking of C-NH_2 bond, is not a primary step in agreement with electronic density.

In the case of photocatalytic degradation of uracil, the formation of nitrate and of ammonium ions occurs only after total disappearance of uracil ([uracil = 245 μmol L^{-1}]). After an irradiation time of 20 h about 98% of nitrogen mineralization was observed. The more important formation of NO_3^- ions is in agreement with the work of Horikoshi et al. [16] and of Pelizzetti et al. [34]. Actually, the latter authors considered that the presence of a carbonyl group near the amine group (case of urea or of formamide) favours the formation of nitrate ions.

3.5. Organic compounds

In order to better understand the different steps of the degradation of pyrimidine compounds, the formation of organic intermediate compounds are followed in the photocatalytic degradation of uracil and of cytosine.

Fig. 11a and b presents a chromatogram obtained after 30 min of degradation of both molecules. First of all, we noticed that uracil is not an intermediate compound of cytosine degradation. This results is in agreement with the formation of NH_4^+ and the electronic density indicating that C-NH_2 oxidation is not a primary step. The first step should be hydroxylation of carbon C2.

Secondly, we observed that five identical compounds (A, B, C, D and F) are found in the degradation of both molecules. However, only three are identified: oxalic acid (peak A), tartronic acid (HOOC-CH(OH)-COOH: peak B) and mesoxalic acid (HOOC-CO-COOH: peak C).

In the degradation of cytosine, lactic acid (CH_3-CH(OH)-COOH: peak G) is detected but not in the degradation of uracil.

The formations of peak A, B and C observed in the degradation of both molecules are given in Fig. 12.

Oxalic acid appears from the beginning and increases until a maximum corresponding to the time necessary to the complete disappearance of cytosine and of uracil in solution. The five other acids are not primary products. The organic carbon coming from these different acids has been compared to the experimental TOC found in solution (Fig. 7). It is interesting to notice that after the total disappearance of uracil and of cytosine, about 80% of the organic matter comprises from acid compounds.

All the other organic compounds detected were not identified. However, considering the electronic density given in Table 3 and the presence of peak D and F similar for both molecules but not identified, we propose that these two compounds could correspond to 2-hydroxy uracil and 2,3-dihydroxyuracil.

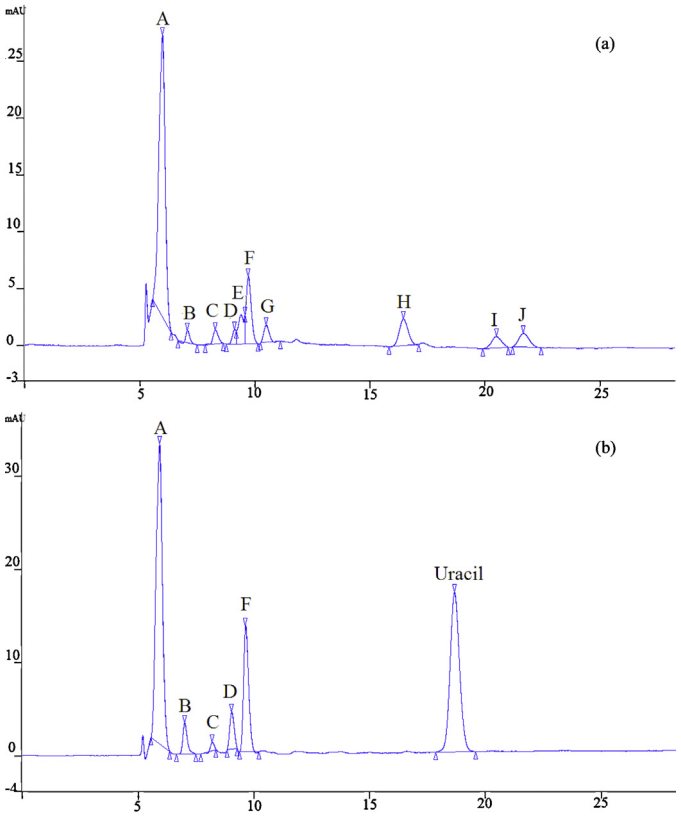

Fig. 11. Chromatogram of intermediate compounds formed after 30 min of degradation of (a) cytosine and (b) uracil.

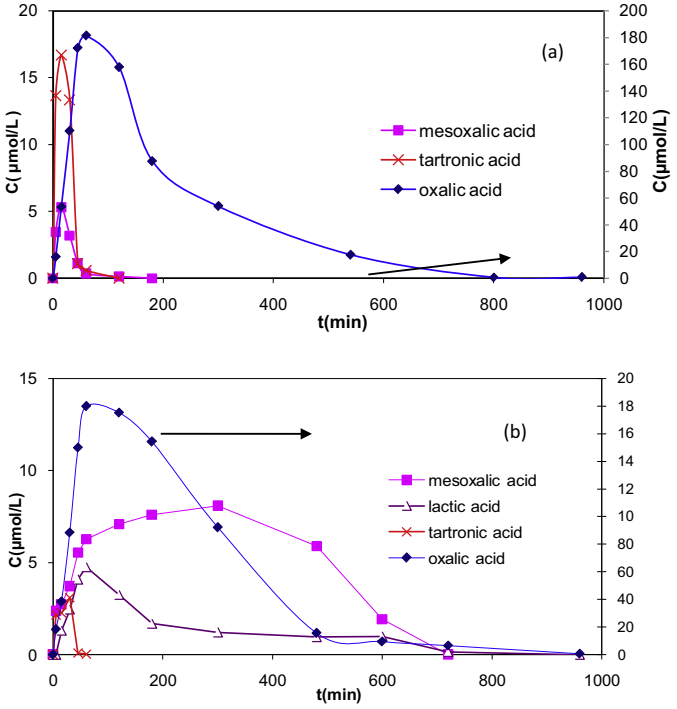

Fig. 12. Formation of oxalic, tartronic and mesoxalic acids during the photocatalytic degradation of uracil (a) and cytosine (b)

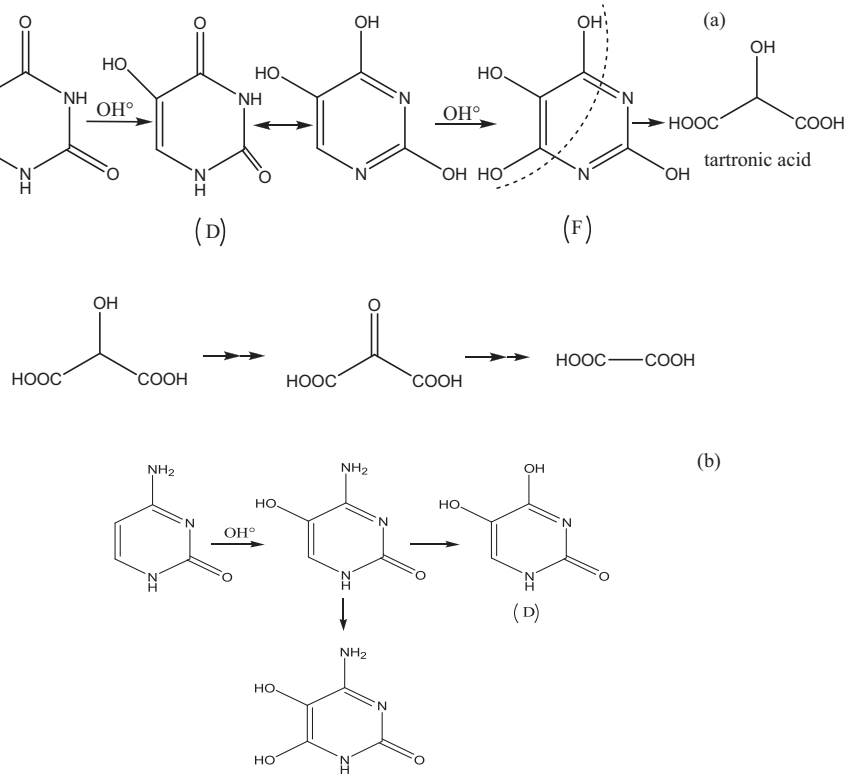

Fig. 13. Tentative chemical pathways for uracil (a) and cytosine (b) photocatalytic degradation.

A suggesting relating to one step of degradation of uracil and cytosine is presented in Fig. 13.

4. Conclusion

The adsorption constants of cytosine and of uracil in the dark and under irradiation, given by the Langmuir and Langmuir–Hinshelwood models respectively, showed a modification of the coverage of cytosine under UV-A irradiation, whereas that of uracil was not modified. This behaviour has been explained considering the positive charge of cytosine at neutral pH (pH 5) which can influence the adsorption constant due to the ionisation of TiO_2 surface under irradiation whereas neutral form of uracil is always present.

At the same coverage, a higher amount of cytosine has been detected on TiO_2 leading to a higher disappearance rate. However, a lower mineralization rate of cytosine was observed indicating that the disappearance rate was not sufficient to estimate the efficiency of photocatalytic process.

The formation of NH_4^+ and NO_3^- ions has been found to be dependent upon the existence of the carbonyl and of the amine groups on the pyrimidine cycles. A more important formation of NO_3^- ions has been observed for uracil having the carbonyl group. By contract, the main inorganic nitrogen ions formed was NH_4^+ ions in the case of cytosine bearing a primary amine function.

The electronic density, the fate of nitrogen and the study of organic intermediates allowed us to propose a chemical pathway. The initial attack of the OH radicals was not found to be on the carbon atom bearing the NH_2 group. Actually, uracil is not a degradation product of cytosine and NH_4^+ ions are not formed from the beginning of degradation. The first attack of OH radicals was observed on the two carbons atoms of the double bond due to their highest electronic density. The attack of OH radicals on the carbon atom bearing the NH_2 substituent leads to the formation of five identical intermediates in cytosine and uracil degradation, which are oxalic, tartronic, mesoxalic acids and mono and di-hydroxy uracil.

This type of study is important to understand the potential applications of photocatalysis in the “bioworld” such as disinfection, sterilization and degradation of biomolecules such as DNA and RNA as well as undesirable organic aqueous pollutants.

References

[1] J.P. Percherancier, R. Chapelon, B. Pouyet, J. Photochem. Photobiol. A: Chem. 87 (1995) 261–266.
[2] L. Amalric, C. Guillard, P. Pichat, J. Photochem. Photobiol. A: Chem. 85 (1995) 257–262.
[3] A. Mills, P. Sawunyama, J. Photochem. Photobiol. A: Chem. 84 (1994) 305–309.
[4] H.Y. Chen, O. Zabraa, M. Bouchy, F. Thomas, J.Y. Bottero, J. Photochem. Photobiol. A: Chem. 85 (1995) 179–186.
[5] N. Serpone, R.F. Khairutdinov, Stud. Surf. Sci. Catal. 103 (1997) 417–444.
[6] C. Anderson, A.J. Bard, J. Phys. Chem. 99 (1995) 9882–9885.
[7] K.S. Jung, H.-I. Lee, J. Korean Chem. Soc. 41 (1997) 682–684.
[8] H.S. Lee, T. Hur, S. Kim, J.H. Kim, H.I. Lee, Catal. Today 84 (2003) 173–180.
[9] M.R. Dhananjeyan, R. Annapoorani, S. Lakshmi, R. Renganathan, J. Photochem. Photobiol. A: Chem. 96 (1996) 187–191.
[10] M.R. Dhananjeyan, R. Annapoorani, R. Renganathan, J. Photochem. Photobiol. A: Chem. 109 (1997) 147–153.
[11] M.R. Dhananjeyan, V. Kandavelu, R. Renganathan, J. Mol. Catal. A: Chem. 151 (2000) 217–223.
[12] G. Plantard, T. Janin, V. Goetz, S. Brosillon, Appl. Catal. B: Environ. 115–116 (2012) 38–44.
[13] H. Cao, X. Lin, H. Zhan, H. Zhang, J. Lin, Chemosphere 90 (2013) 1514–1519.
[14] H. Hou, X. Wang, C. Chen, D.M. Johnson, Y. Fang, Y. Huang, Catal. Commun. 48 (2014) 65–68.
[15] G. Li, X. Liu, T. An, H. Yang, S. Zhang, H. Zhao, Catal. Today (2014), in press.
[16] S. Horikoshi, N. Serpone, S. Yoshizawa, J. Knowland, H. Hidaka, J. Photochem. Photobiol. A: Chem. 120 (1999) 63–74.
[17] J.L. Lucas Vaz, A.Y. Boussaoud, Y. Ait Ichouet, M. Petit-Ramel, Analusis 26 (1998) 83–87.
[18] C. Jaussaud, O. Païssé, R. Faure, J. Photochem. Photobiol. A: Chem. 130 (2000) 157–162.
[19] H.K. Singh, M. Saquib, M.M. Haque, M. Muneer, J. Hazard. Mater. 142 (2007) 425–430.
[20] M. El Madani, C. Guillard, N. Peírol, J.M. Chovelon, M. El Azzouzi, A. Zrineh, J.M. Herrmann, Appl. Catal. B: Environ. 65 (2006) 70–76.
[21] H.P. Boehm, M. Herrmann, Z. Anorg. Allg. Chem. 352 (1967) 156–167.
[22] L. Elsellami, F. Vocanson, F. Dappozze, R. Baudot, G. Febvay, M. Rey, A. Houas, C. Guillard, Appl. Catal. B: Environ. 94 (2010) 192–199.
[23] L. Elsellami, F. Vocanson, F. Dappozze, E. Puzenat, O. Païsse, A. Houas, C. Guillard, Appl. Catal. A: Gen. 380 (2010) 142–148.
[24] S. Helali, F. Dappozze, S. Horikoshi, T. H-Bui, N. Perol, C. Guillard, J. Photochem. Photobiol. A: Chem. 255 (2013) 50–57.
[25] H. Lachheb, F. Dappozze, A. Houas, C. Guillard, J. Photochem. Photobiol. A: Chem. 246 (2012) 1–7.
[26] A. Turki, C. Guillard, F. Dappozze, G. Berhault, Z. Ksibi, H. Kochkar, J. Photochem. Photobiol. A: Chem. 279 (2014) 8–16.
[27] J. Moreira, B. Serrano, A. Ortiz, H. de Lasa, Chem. Eng. Sci. 78 (2012) 186–203.
[28] G. Marci, A. Sclafani, V. Augugliaro, L. Palmisano, M. Schiavello, J. Photochem. Photobiol. A: Chem. 89 (1995) 69–74.
[29] C. Turchi, D.F. Ollis, J. Catal. 122 (1990) 178–192.
[30] D.F. Ollis, E. Pelizzcni, N. Serpone, Environ. Sci. Tech. 25 (1) (1991) 1523–1529.
[31] H. Hidaka, S. Horikoshi, K. Ajisaka, J. Zhao, N. Serpone, J. Photochem. Photobiol. A:.Chem. 108 (1) (1997) 197–205.
[32] G.J. Fleming, K. Adib, J.A. Rodriguez, M.A. Barteau, J.M.H. White, H. Idriss, Surf. Sci. 602 (2008) 2029–2038.
[33] T.-H. Bui, M. Karkmaz, E. Puzenat, C. Guillard, J.-M. Herrmann, Res. Chem. Intermed. 33 (2007) 421–431.
[34] E. Pelizzetti, P. Calza, G. Mariella, V. Maurino, C. Minero, C. Maurino, H. Hidaka, Chem. Commun. (2004) 1504–1505.